



Published in final edited form as:

Pain. 2022 June 01; 163(6): 1091–1101. doi:10.1097/j.pain.0000000000002511.

Expression of ectopic heat shock protein 90 in male and female primary afferent nociceptors regulates inflammatory pain

Yaomin Wang¹, Scott A Scarneo^{1,2}, Shin Hyung Kim^{1,3}, Xin Zhang¹, Jiegen Chen¹, Kelly W. Yang², Philip Hughes², Timothy Haystead², Andrea G Nackley^{1,2,*}

¹Center for Translational Pain Medicine, Department of Anesthesiology, Duke University School of Medicine, Durham NC 27705

²Department of Pharmacology and Cancer Biology, Duke University School of Medicine, Durham NC 27705

³Department of Anesthesiology and Pain Medicine, Yonsei University College of Medicine, Seoul, Korea

1. Introduction

Chronic pain is a prevalent health concern, affecting up to 100 million people in the US alone, with greater rates of pain reported in females compared to males.[10; 11] The development of chronic pain is driven by multiple signaling pathways linked to heightened nociceptor activity. Emerging data has shown that heat shock protein 90 (Hsp90) is a key regulator of signal transduction events underlying chronic pain and inflammation.[14] Hsp90 is a ubiquitously expressed cellular protein essential for regulating proteomic stress by modulating the tertiary structure of cytosolic proteins, and maintaining their stability in both homeostatic and disease states.[23; 40] To date, only a handful of studies have explored the role of Hsp90 in pain. Hsp90 has been shown to contribute to the pathophysiology of mono arthritis and neuropathic pain through its regulation of TLR4 signaling in DRG, spinal cord, and brain.[14; 22] In line with these findings, inhibition of Hsp90 has been shown to reverse mechanical allodynia and enhance morphine-induced analgesia.[14] However inhibition of Hsp90 has also been shown to block morphine-induced anti-nociception in HIV and cancer pain models primarily through regulation of downstream ERK signaling and protein translation.[32],[18] Thus, Hsp90's role in pain signaling may be context-dependent.

Hsp90 was long thought to be solely expressed intracellularly; however, data in the cancer field has shown that membrane-bound, ectopic Hsp90 (eHsp90) expression can be induced in metastatic tumor cells during disease progression.[4] In metastatic cancer cells eHsp90 has been shown to regulate the expression and signaling of disease-relevant proteins at the cellular membrane. Similar to cancer cells, eHsp90 expression is increased on immune cells following their activation, where it is thought to regulate the rapid increase in membrane-

* **Corresponding author:** Andrea G. Nackley, PhD, Associate Professor, Center for Translational Pain Medicine, Department of Anesthesiology, Duke University School of Medicine, 3 Genome Court, Durham NC 27710, andrea.nackley@duke.edu, Phone: (919) 613-5911, Fax: (919) 613-2324.
Dr. Scott Scarneo and Dr. Yaomin Wang both contributed equally to this manuscript.

bound receptor signaling.[34] Yet, a significant gap remains in our knowledge of eHsp90 on non-cancerous cells in various disease states and no published reports have begun to elucidate the putative role of eHsp90 in pain.

Here, using a cell impermeable eHsp90 inhibitor, we sought to determine the expression of eHsp90 in the peripheral and central nervous system as well as to determine the role of eHsp90 in mediating pain, edema, and nociceptor activity in the complete Freund's adjuvant (CFA) model of inflammation. Our results show that inflammation leads to an upregulation of eHsp90 on DRG nociceptors and that inhibition of eHsp90 reduces nociceptor activity, pain, and inflammation in a sex-dependent manner. Thus, eHsp90 targeted inhibitors may represent novel therapies for the treatment of chronic pain conditions associated with autoimmunity or immune challenge.

2. Materials and Methods

2.1. Animals

For biochemical and behavioral experiments, adult male (N=69) and female (N=87) C57/BL6 mice weighing ~18–23 grams were bred in-house or purchased from The Jackson laboratory (Bar Harbor, ME, USA). For calcium imaging experiments, adolescent male (N=15) and female (N=10) Pirt-GCaMP3 mice weighing ~18–23 grams were bred in-house. Mice were housed in a temperature- and humidity-controlled facility maintained under 12-hour light/dark cycle (lights on at 7 am) and had access to food and water *ad libitum*. All procedures were approved by the Duke University Institutional Animal Care and Use Committee (IACUC) and conformed to the National Institutes of Health Guide for the Care and Use of Laboratory Animals[43] and the Animal Research: Reporting of In Vivo Experiments guidelines.[24]

2.2. CFA model of inflammation

Mice were gently restrained, and separate groups received a unilateral intraplantar (i.pl.) injection of CFA (25 μ L) or incomplete Freund's adjuvant (IFA; 25 μ L). In all studies, the experimenter was blinded to the treatment conditions.

2.3. Whole body cryo-imaging

HS-131 is a well-established selective non-cell permeable eHsp90 fluor-inhibitor consisting of an Hsp90-binding ligand, a polyethylene-based tether (linker), and a fluorophore (Cy5 dye ex640nm/em680nm) (Fig 1A).[7; 13] HS-198 is a control molecule, where substitution of a N'N dimethylamide to the Hsp90 ligand renders it inactive. Following cellular upregulation of eHsp90, HS-131 can bind membrane expressed Hsp90 and subsequently be internalized into the intracellular space (Fig 1B). On day 3 following i.pl. CFA, separate mice received either HS-131 (10 nmoles i.v.) or HS-198 (10 nmoles i.v.) and were fixed for whole body cryo-imaging 6 hours later. Mice were serially imaged at 10.23 μ m \times 10.23 μ m in-plane resolution by an Olympus MVX-10 microscope with a 1X objective, 0.63X magnification and 40 μ m section thickness, using the CryoViz™ (BioInVision, Inc., Cleveland, OH, USA). Individual slices were captured using a dual band FITC/TxRed fluorescence filter (Chroma, Inc., Rockingham, VT, USA), a liquid crystal RGB filter and a

low-noise monochrome camera. Raw images were reconstructed using Imaris 9.5 software to generate 3D pictures and videos.

2.4. Immunohistochemical and fluorotag staining

On day 3 following i.pl. CFA or IFA administration, mice were deeply anesthetized with an intraperitoneal injection of 300mg/kg Fatal Plus (Vortech Pharmaceuticals, Dearborn, MI, USA), and subsequently perfused intracardially with 50 mL of ice-cold heparinized 0.1 M phosphate-buffered saline. This was followed by 25–50 ml fixative (4% paraformaldehyde in 0.1 M sodium phosphate buffer). The DRG were isolated, post-fixed in 4% paraformaldehyde for 12 hr, and finally immersed in a 30% sucrose solution for storage at 4°C until sectioning. Transverse sections were cut to a thickness of 10 μm , incubated in 5% fetal bovine blocking serum in 0.01 M phosphate-buffered saline at room temperature for 1 hr, and stained overnight at 4°C with primary antibodies for anti-rabbit Hsp90 (1:1000; Cell Signaling, USA), anti-mouse GFPA (1:1000; Millipore, US), and anti-rat CD68 (1:1000, Bio-rad, US). The following day, the sections were incubated with corresponding secondary antibodies or NeuroTrace™ fluorescent Nissl (1:500, Invitrogen, US) for 1 hr at room temperature. The specificity of immunohistochemical staining was verified by omission of the primary antibody or omission of the secondary antibody from the staining protocol for each set of experiments. Histological features of DRG were captured using a Zeiss 880 confocal microscope (Germany). Hsp90 protein expression was determined for 3 different cell areas (<400 μm^2 for small, 400 – 900 μm^2 for medium, >900 μm^2 for large). Image J was used for Hsp90 intensity quantification.

eHsp90 expression was evaluated in female mice DRG six hours post HS-131 treatment (10 nmoles, i.v.) on day three following intra-plantar CFA injection. Briefly, mice were perfused with 1XPBS immediately following sacrifice, followed perfusion in 4% paraformaldehyde solution. DRG were isolated and stored in a 30% sucrose solution overnight at 4°C overnight. Transverse sections were cut to a thickness of 12 μm , placed on a tissue slide. Images were captured using a Zeiss 880 confocal microscope (Germany).

2.5. Western blot analysis

Affected L4–6 DRG and un-affected C5–7 DRG were harvested from CFA or IFA mice on day 3. The Mem-PERTM Plus Membrane Protein Extraction Kit (89842, Thermo Scientific, US) was used to separate membrane and cytosolic protein fractions. Briefly, the homogenized DRG lysates were permeabilized with a mild detergent to allow the release of soluble cytosolic proteins, then a second detergent was used to solubilize membrane proteins. Protein concentrations were normalized by bicinchoninic acid (BCA; Pierce, Grans Island, NY, USA) measurement. Gels were run using the standard SDS-PAGE method and transferred onto PVDF membranes using an iBlot2 dry blotting system (Life Technologies). Membranes were then blocked, probed with primary antibodies for Hsp90 (1:1000; Cell Signaling, USA), Na⁺-K⁺-ATPase (1:1000; Cell Signaling, USA), and GAPDH (1:1000; Cell Signaling, USA), and finally probed with corresponding secondary antibodies. Specific bands were visualized with enhanced chemiluminescence (Thermo Scientific, USA) and quantified using Image J. The relative levels of membrane and cytosolic Hsp90 proteins were normalized to Na⁺-K⁺-ATPase and GAPDH, respectively.

2.6. Hsp90 Purification

Hsp90 was purified from C57/Bl6 livers via Hsp90 affinity resins. Mouse livers were dissected from mice immediately following sacrifice, mechanically dissociated through a 0.22 μ m filter and lysed in 30 mM Tris-HCl, pH 7.5, 1 mM EGTA, 1 mM EDTA, 150 mM NaCl, 0.2 mM DTT with protease inhibitors solution. 3 mL of lysis supernatant was loaded onto 2 mL of selective Hsp90 affinity resin. [13] The resin-cell lysis mixture was placed on a rocker at 4°C for 45 mins. This was followed by a sequence of four washes in low salt wash buffer (LSWB; 150 mM NaCl, 25 mM Tris pH 7.5, and 60 mM MgCl₂), two washes in high salt wash buffer (HSWB; 1 M NaCl, 25 mM Tris pH 7.5, 60 mM MgCl₂, and 1 mM DTT) and two in LSBW. Purified Hsp90 was eluted from the resin by 1 μ mol HS-10, verified by silver stain and stored at -20°C.

2.7. Calcium imaging

Calcium imaging was conducted in primary DRG neurons from Pirt-GCaMP3 mice at room temperature.[1] DRG were removed aseptically from euthanized mice and incubated with collagenase (1.25 mg/mL)/dispase-II (2.4 units/mL) at 37°C for 120 min, then digested with 0.25% trypsin for 8 min at 37°C, followed by 0.25% trypsin inhibitor. Cells were mechanically dissociated with a flame polished Pasteur pipette in the presence of 0.05% DNase I. DRG cells were plated on glass coverslips and grown in a neurobasal defined medium with 2% B27 supplement and 5 mM AraC maintained in a 5% CO₂ incubator at 37°C. DRG neurons were grown for 24 hr before use. The calcium imaging buffer included 140 mM NaCl, 10 mM D-(+)-Glucose, 1 mM MgCl₂, 2 mM CaCl₂, 5 mM KCl, 10 mM HEPES, pH = 7.4, osmolarity = 320 mOsm/L. Calcium signals were measured using green emitted light in a 3 s interval. To evaluate the effect of Hsp90 on calcium responses, 3 different doses of Hsp90 (0.5, 1.5, and 5.0 μ g/mL, diluted in calcium imaging buffer) were prepared and each delivered to a separate coverslip of DRG cells for 2 min. To determine the effect of HS-131 on Hsp90-induced calcium responses, 3 different doses of HS-131 (0.01, 0.05, and 1.0 μ M, diluted in DMSO solution) were prepared and each loaded onto a separate coverslip of DRG cells for 2 min prior to delivery of 5.0 μ g/mL Hsp90. To evaluate the effects of female hormones on Hsp90-induced calcium responses, 1 ng/ml of 17 β -estradiol (E2) was administrated to male DRG cells for overnight incubation. Calcium signal amplitudes representing Calcium influx intensity change were presented as $DF/F_0 = (F_t - F_0)/F_0$ as ratio of fluorescence difference ($F_t - F_0$) to basal value (F_0). The average fluorescence intensity in the baseline period was taken as F_0 .

2.8 Systemic Hsp90 challenge

Male and female mice were gently restrained, and received tail vein injections (i.v.) of Hsp90 (10, 20 or 40 μ g/mouse). Mechanical allodynia and mechanical hyperalgesia were evaluated prior to (baseline) and at 1, 3 and 6 hours post injection. Thermal hyperalgesia was evaluated prior to and 6 hours post injection.

2.9. Pain behavior testing

In general, male and female mice were handled and habituated to the testing environment for 3 days prior to random assignment to one of four experimental groups: CFA+Vehicle,

CFA+HS-131, IFA+Vehicle, or IFA+HS-131. Pain behaviors evoked by mechanical and thermal stimuli were evaluated on day 0 prior to and on days 1, 2, and 3 following administration of CFA or IFA. On day 3, behaviors were re-evaluated following treatment with HS-131 (or HSP90) or vehicle at 1, 3, and 6 hours.

Paw withdrawal thresholds were determined using the von Frey up-down method.[8] Mice were placed in clear Plexiglas chambers with a wire mesh floor and allowed to habituate for 30 minutes. Testing was conducted using a series of nine von Frey monofilaments with logarithmically increasing stiffness (0.02–2.56g, North Coast Medical, CA) presented perpendicularly to the central plantar surface of the hindpaw. First, the middle filament (0.4 g) was applied to the hindpaw for 2 s. If the mouse responded with a withdrawal, an incrementally lower filament was applied. In the absence of a withdrawal, an incrementally higher filament was applied. A series of six total responses were recorded for each paw. Results were determined using a logarithmic algorithm to determine the gram-force value that would elicit paw withdrawal in 50% of trials ($10^{[Xf + k\delta]}/10,000$), where Xf = value of final von Frey hair used (log units); k = tabular value of X (positive) and O (negative) responses; δ = mean difference between stimuli (log units). Mechanical allodynia was defined as a significant decrease in paw withdrawal threshold from baseline

After determining paw withdrawal threshold, paw withdrawal frequency to a noxious von Frey monofilament was assessed. A supra-threshold filament (0.4 g) was applied to the hindpaw 10 times for a duration of 1s, with a 1s interval between stimuli. Mechanical hyperalgesia was defined as a significant increase in the number of paw withdrawals from baseline.

Finally, paw withdrawal latency to thermal heat was assessed using the Hargreaves method. [12] Mice were placed in plexiglass chambers on a glass table and habituated for 30 minutes. A heat source was positioned under the glass directly beneath the hind paw to obtain withdrawal latencies. A maximal cut-off of 20 seconds was utilized to prevent tissue damage. Paw withdrawal latencies were recorded in duplicate per paw. If the second latency recorded was not within ± 4 seconds of the first, a third measure was recorded. The two latencies closest in value were averaged to determine overall latency to withdrawal. Thermal hyperalgesia was defined as a decrease in paw withdrawal latency from baseline.

2.10. Motor function and hindpaw edema assessment

On day 3 following CFA administration, motor function was evaluated prior to and 6 hours following HS-131 or vehicle treatment using a Rota-rod system (IITC Life Science Inc.). Each test consisted of 3 trials separated by 10 min intervals, during which the speed of rotation accelerated from 4 to 40 rpm in 5 min. The falling latency was recorded.[42] Also, on day 3 following CFA administration, hindpaw diameter (mm) was measured prior to and 6 hours following HS-131 or vehicle treatment using a caliper.

2.11. Statistical analysis

GraphPad Prism 9 was used for statistical analysis of all data. Immunohistochemical, calcium imaging, and behavioral data were evaluated by 1-way or 2-way ANOVA to identify main effects followed by Dunnett's multiple comparison test to identify specific group

differences. Western blot data were analyzed by two-tailed t-test. An alpha of 0.05 was considered statistically significant.

3. Results

3.1. Intraplantar CFA induces eHsp90 expression on primary afferent nociceptors in DRG

Here, we sought to characterize the expression of membrane bound eHsp90 in a mouse CFA model of inflammation and determine its role in nociception and inflammatory pain. First, we examined global expression of eHsp90 by whole body cryo-imaging mice injected with the selective non-cell permeable eHsp90 fluor-inhibitor HS-131 or the inactive control HS-198 on day 3 following intraplantar CFA. Biodistribution of HS-131 was observed by histological examination of individual slices and after *in silico* reconstruction of the entire mouse anatomy (Movie S1). Examination of the *in silico* mouse reconstruction showed fluorescence in the hepatobiliary and intestinal tissues, consistent with the previously observed mechanisms of clearance HS-131 *in vivo*. [7] Comparison of HS-131- to HS-198-treated mice shows that CFA induced robust eHsp90 expression in lumbar DRG (Fig 2A). Further histological analysis demonstrates that expression is highest in L3-L5 DRG, with no difference between those ipsilateral and contralateral to the CFA injection site (Fig 2B).

The DRG is vast network of cells comprised of neurons, glia, and immune cells, all of which influence nociception. [28] Thus, we evaluated the expression of Hsp90 in these cellular populations following intraplantar CFA. Immunohistochemical analysis of DRG isolated on day 3 post-CFA show that Hsp90 is localized to Nissl+ neurons, with minimal to no expression in GFAP+ satellite glia or CD68+ monocytes/macrophages (Fig 2C). Consistent with cryo-imaging results, Hsp90 expression levels were comparable between ipsilateral and contralateral DRG neurons (Fig 2D). Control animals injected with IFA showed similar staining patterns in the DRG, with Nissl+ neurons showing robust expression of Hsp90 (Fig S1A). Additionally, due to the lack of eHsp90 discriminant antibodies, we performed fluorescence staining on L4 DRG on day 3 post CFA following HS-131 i.v. injection. Immunohistochemical analysis of the DRG (Fig S1B) showed similar staining patterns as observed in Fig 2.

3.2. CFA-induced eHsp90 expression in lumbar DRG is greater in females.

Next, we examined expression of eHsp90 in membrane versus Hsp90 in cytosolic fractions of DRG nociceptors collected from male and female mice on day 3 post-CFA. Western blot analysis of these fractions showed that eHsp90 expression was higher in membranes isolated from lumbar DRG innervating the affected hind paw compared to membranes isolated from cervical DRG innervating unaffected remote sites for both males ($t_{12} = 3.55$, $P < 0.01$) and females ($t_{12} = 4.14$, $P < 0.001$; Fig 3A). Notably, compared to males, females exhibited significantly higher levels of eHsp90 expression in membranes from lumbar DRG ($t_{12} = 2.42$; $P < 0.05$). No differences in cytosolic Hsp90 expression were found between lumbar and cervical DRG or between males and females (Fig 3B). Furthermore, no differences in eHsp90 expression were observed in cervical or lumbar DRG collected from control male and female mice on day 3 post-IFA (Fig S2).

3.3. Exogenous Hsp90 induces nociceptor activity and pain, which is greater in females.

To directly test the effect of increased Hsp90 levels on nociceptor activity, we used primary DRG neurons isolated from Pirt-GCaMP3 mice which express a fluorescent calcium indicator in response to activating ligands.[1] In mixed primary neurons isolated from both male and female Pirt-GCaMP3 mice, we observed a dose-dependent increase in calcium response following administration of 0.5, 1.5, and 5.0 $\mu\text{g/ml}$ Hsp90 ($F_{3, 1489} = 95.52$, $P < 0.001$; Fig 4A).

Due to our observed sex differences in eHsp90 expression, we next evaluated Hsp90-induced calcium responses in separate DRG isolated from either male or female Pirt-GCaMP3 mice in the presence or absence of HS-131. Administration of Hsp90 (5 $\mu\text{g/mL}$) to male- and female-isolated primary neurons induced significant increases (60% and 80%, respectively) in male (Fig 4B) and female (Fig 4C) DRG calcium responses that were dose-dependently decreased by HS-131. Treatment with the high 1 μM dose of HS-131 more effectively attenuated calcium responses in male compared to female-isolated neurons.

To determine if the exaggerated Hsp90-induced calcium signaling in female-isolated DRG neurons is dependent on sex hormones, we treated male-isolated primary neurons with varying concentrations of the female hormone estrogen as previously described.[41] We found that male-isolated neurons exhibited dose-dependent increases in Hsp90-induced calcium response following overnight incubation with 1.0, 3.0, or 30.0 ng/ml estrogen compared to naïve male neurons ($F_{4, 2609} = 6.26$, $P < 0.0001$, $n=10$; Fig 4C).

We next tested the effects of systemic Hsp90 administration (10, 20, or 40 μg , i.v.) in male and female mice. In male mice, the 40 μg dose directly induced mechanical allodynia ($F_{9, 42} = 2.22$, $P = 0.04$) and mechanical hyperalgesia ($F_{9, 42} = 2.55$, $P = 0.02$), but not thermal heat hyperalgesia within 3–6 hours (Fig S3). In female mice, the 10, 20, and 40 μg doses directly induced mechanical allodynia ($F_{9, 42} = 3.90$, $P = 0.001$) and mechanical hyperalgesia ($F_{9, 42} = 5.33$, $P < 0.0001$), and the 40 μg dose induced thermal heat hyperalgesia ($F_{3, 14} = 9.09$, $P = 0.001$) within 3–6 hours.

3.4. The eHsp90 inhibitor HS-131 reverses CFA-induced mechanical and thermal pain, with females requiring a higher dose

Finally, we sought to determine the therapeutic potential of eHsp90 inhibition on pain behavior *in vivo*. As illustrated in Figure 5A, behavioral responses were evaluated in separate groups of male and female mice treated with HS-131 (10 nmoles) or vehicle on day 3 following i.pl. injection of CFA or IFA. Consistent with previous literature, both male and female mice showed robust CFA-dependent mechanical allodynia ($F_{3, 90} = 22.27$, $P < 0.0001$ for males, $F_{3, 99} = 9.29$, $P < 0.0001$ for females), mechanical hyperalgesia ($F_{3, 90} = 17.21$, $P < 0.0001$ for males, $F_{3, 99} = 8.53$, $P < 0.0001$ for females), and thermal heat hyperalgesia ($F_{3, 90} = 6.21$, $P = 0.0007$ for males, $F_{3, 99} = 4.89$, $P = 0.004$ for females) in their injected hindpaws on days 1–3 compared to baseline, while i.pl. IFA had no effect (Fig S4).[25] In line with our finding that Hsp90 is expressed in DRG innervating the hindpaw contralateral as well as ipsilateral to the CFA injection site, female mice also showed CFA-dependent mechanical allodynia ($F_{3, 99} = 6.80$, $P = 0.0003$), mechanical hyperalgesia ($F_{3, 99} = 5.80$,

$P = 0.001$), and thermal heat hyperalgesia ($F_{3, 99} = 6.63$, $P = 0.0004$) in their non-injected hindpaws on days 1–3 compared to baseline (Fig S5). Male mice showed similar trends towards CFA-dependent increases in mechanical and thermal pain in their non-injected hindpaws, although not significant. In male mice, administration of HS-131 (10 nmol) on day 3 reversed CFA-dependent mechanical allodynia ($F_{9, 81} = 2.00$, $P = 0.04$) measured at 1, 3, and 6 hours post-treatment, mechanical hyperalgesia ($F_{9, 81} = 2.76$, $P = 0.007$) measured at 3 and 6 hours post-treatment, and thermal heat hyperalgesia ($F_{3, 25} = 10.73$, $P = 0.0001$) measured at 6 hours post-treatment (Fig 5B). In female mice, however, administration of HS-131 (10 nmol) failed to significantly reduce mechanical and thermal pain (Fig 5C).

A signature feature of the CFA inflammatory model is the induction of edema within the intraplantar space, with the expression of inflammatory mediators leading to heightened nociceptor activity.[9] Previous literature has shown that inhibition of Hsp90 on activated innate and adaptive immune cells can block functional responses such as release of cytokines.[29],[20],[26],[39],[6] To evaluate the effects of systemic eHsp90 inhibition on hindpaw edema, we measured paw diameter in mice receiving HS-131 or vehicle on day 3 following i.pl. injection of CFA or IFA. In male mice, administration of HS-131 (10 nmol) significantly reduced hindpaw edema by ~15% 6-hour post-treatment ($F_{3, 16} = 5.41$, $P < 0.01$; Fig 5B). In female mice, however, administration of HS-131 had no effect on hind paw edema (Fig 5C).

As female mice express significantly more eHsp90 on primary afferent neurons than do males as well as heightened response to systemic Hsp90 delivery we next tested a higher (20 nmol) dose of HS-131 in the CFA model. Indeed, treatment of female mice with 20 nmol HS-131 significantly reversed mechanical allodynia ($F_{3, 27} = 15.32$, $P < 0.0001$) and mechanical hyperalgesia ($F_{3, 27} = 40.05$, $P < 0.0001$) at 1, 3 and 6 hours as well as thermal heat hyperalgesia at 6 hours ($t_9 = 3.01$, $P < 0.02$) (Figure 6A–C). Further, treatment of female mice with 20 nmol HS-131 significantly reduced CFA-induced hindpaw edema measured 6 hours later ($t_9 = 3.01$, $P = 0.01$) (Figure 6D).

Finally, as eHsp90 inhibitors represent a novel class of potential analgesics, we evaluated the effects of HS-131 on motor function in male and female mice. Compared to vehicle, administration of HS-131 had no effect on fall latency measured at 6 hours post-treatment in either male or female mice (Fig S6).

4. Discussion

Emerging evidence suggests that Hsp90 regulates critical signaling pathways underlying chronic pain, yet the role of the membrane-bound eHsp90 form in this pathway, if any, has remained undetermined. Here, using HS-131, a cell impermeable eHsp90 inhibitor, we provide the first demonstration that eHsp90 plays a key role in the pathogenesis of inflammatory pain. We found that inflammation leads to an upregulation of eHsp90 on DRG nociceptors, with higher levels observed in females. Further, we found that inhibition of eHsp90 reduces nociceptor activity, pain, and inflammation in a sex-dependent manner, such that females require higher dosing with the selective eHsp90 inhibitor HS-131.

4.1 CFA induces eHsp90 expression on DRG nociceptors, where it acts to increase calcium responses.

Previous studies have shown that eHsp90 is upregulated in tumor cells undergoing metastatic progression, and it is thought to stabilize oncogene driven client proteins and receptors in the cell membrane.[2; 3; 17] Here, using the eHsp90 selective fluor-inhibitor HS-131 we show that eHsp90 is upregulated on the cell bodies of primary afferent nociceptors located in L3-L5 DRG on day 3 following intraplantar CFA injection. Western blot analysis of these fractions confirmed that CFA-induced increases in Hsp90 were localized to the membrane and not the cytosol. Of note, increased eHsp90 expression was observed in lumbar DRG contralateral as well as ipsilateral to the site of CFA injection. Contralateral expression of eHsp90 in lumbar DRG is unlikely due to a lack of specificity of HS-131 or the Hsp90 antibody, as only minimal expression was observed in cervical DRG with no difference between CFA and IFA groups. It is possible that cleaved eHsp90 from ipsilateral DRG is stimulating nociceptor activity via ectopic Hsp90 secretion and stimulation of adjacent contralateral DRG; however further experimental studies would be needed to more fully define this hypothesis.[31]

To directly test the effect of increased eHsp90 levels on nociceptor activity, we used primary DRG neurons isolated from Pirt-GCaMP3 mice which express a fluorescent calcium indicator in response to activating ligands.[1] In mixed primary neurons isolated from both male and female Pirt-GCaMP3 mice, we observed a dose-dependent increase in calcium response following administration of Hsp90. This finding is in line with those demonstrating that exogenous Hsp90 can bind and activate signaling pathways such as ERK and MAP,[5; 30; 33; 36] which are known to promote increased nociceptor activity and pain.[15; 16]

4.2 Hsp90 expression and activity is greater in female versus male nociceptors.

The effects of Hsp90 may be potentiated by sex hormones such as estrogen, based on our results showing 1) CFA-induced increases in membrane-bound eHsp90 were significantly greater in lumbar DRG isolated from female compared to male mice, 2) female nociceptors and estrogen-treated male nociceptors showed enhanced activity to exogenous Hsp90 stimuli relative to untreated male nociceptors, and 3) systemic delivery of Hsp90 induced greater pain behavior in female compared to male mice. Based on these collective findings it is possible that estrogen increases eHsp90 expression on neurons, which then chaperones critical pro-nociceptive and pro-inflammatory proteins in the membrane leading to heightened nociceptive responses in females. In fact, it has been shown that Hsp90 is expressed in the membrane and forms a functionally integral component of the TLR4 signaling complex, subsequently influencing cellular response to extracellular inflammatory signaling. [35] Although the exact membrane clients of Hsp90 in nociceptors is still unknown, we predict Hsp90 stabilizes several membrane bound proteins involved in pain transmission. Future experiments are needed to truly elucidate the specific mechanism(s) whereby eHsp90 and estrogen network to induce inflammatory pain.

4.3 eHsp90 inhibition reduces nociceptor activity, pain, and inflammation, with females requiring higher doses of HS-131.

After demonstrating CFA-induced eHsp90 expression is localized to DRG neurons, where it promotes increases in their calcium-dependent activity, we next sought to test the effects of the specific eHsp90 inhibitor HS-131 on nociception, pain, and inflammation. In primary DRG neurons isolated from Pirt-GCaMP3 mice, we found that HS-131 dose-dependently decreased Hsp90-induced calcium responses. In line with the finding that Hsp90-induced responses were greater in females than males, we observed that treatment with the high 1 μ M dose of HS-131 more effectively attenuated calcium responses in male compared to female-isolated neurons.

Next, in mice, we found that HS-131 (10 nmols) attenuated mechanical pain, thermal pain, and inflammation in male, but not female mice. Based on the higher expression profile of eHsp90 in female mice, we treated a separate cohort of females with a higher dose HS-131 (20 nmols), after which we observed significant reductions in pain and inflammation. Together, results from both *in vivo* and *ex vivo* experiments support that eHsp90 regulates signaling of proteins in pathways associated with inflammatory pain. In addition, our data suggest that expression of hormones such as estrogen in female nociceptors may increase the expression of eHsp90, leading to a higher drug concentration needed to attenuate eHsp90 signaling in females.

Previous groups have evaluated the therapeutic potential of Hsp90 inhibition in multiple animal models of pain.[22],[19] Hsp90 inhibition as a whole has generally shown robust attenuation of pain in these models however the proposed mechanism of how Hsp90 influences pain has been vast. For example, one group has shown that Hsp90 can regulate TLR4 receptor signaling, where Hsp90 enhanced TLR4 mediated inflammatory nociception leading to an increase in pain like behaviors in rats. [14] In addition to Hsp90 regulation of inflammatory processes that underlie pain, our group and others have shown that Hsp90 inhibition in nociceptors can reduce pain like behaviors. For example, the development of C terminal targeted Hsp90 inhibitors have been shown to block the development of peripheral diabetic neuropathies by blocking neuronal apoptosis, improving mitochondrial function as well as sensory fiber recovery. [37; 38] Ultimately our results and that of others support the continued investigation of Hsp90 as a novel analgesic target for the treatment of a wide array of pain syndromes.

4.4 eHsp90 represents a novel therapeutic target for the treatment of pain.

Current treatments for chronic pain include conventional nonsteroidal anti-inflammatory drugs (e.g., aspirin and ibuprofen), which are short-acting and fail to alleviate severe chronic pain, as well as longer-acting centrally-targeted therapies (e.g., opioids, antidepressants, and anticonvulsants) that show poor efficacy for managing chronic pain and produce adverse side-effects, such as altered mental state, addiction, and respiratory depression.[27],[21] Here, we show that CFA induces eHsp90 expression on nociceptors which may then promote increases in their activity so as to drive nociception and pain. Further, selective inhibition of eHsp90 reduces nociceptor activity and alleviates pain and inflammation. These results support the therapeutic role of targeting eHsp90 in inflammatory pain syndromes. To

date, multiple Hsp90 inhibitors have been clinically developed and tested where they have been well-tolerated in patients. In conclusion, our results show that Hsp90, and in particular eHsp90, regulates critical signaling pathways that underlie the etiology of inflammatory pain and may represent a novel, safe, and effective therapeutic target for patients with chronic pain conditions linked to abnormalities in immune signaling.

Supplementary Material

Refer to Web version on PubMed Central for supplementary material.

Citations

- [1]. Anderson M, Zheng Q, Dong X. Investigation of Pain Mechanisms by Calcium Imaging Approaches. *Neurosci Bull* 2018;34(1):194–199. [PubMed: 28501905]
- [2]. Barrott JJ, Haystead TA. Hsp90, an unlikely ally in the war on cancer. *FEBS J* 2013;280(6):1381–1396. [PubMed: 23356585]
- [3]. Barrott JJ, Hughes PF, Osada T, Yang XY, Hartman ZC, Loiselle DR, Spector NL, Neckers L, Rajaram N, Hu F, Ramanujam N, Vaidyanathan G, Zalutsky MR, Lyerly HK, Haystead TA. Optical and radioiodinated tethered Hsp90 inhibitors reveal selective internalization of ectopic Hsp90 in malignant breast tumor cells. *Chem Biol* 2013;20(9):1187–1197. [PubMed: 24035283]
- [4]. Becker B, Multhoff G, Farkas B, Wild PJ, Landthaler M, Stolz W, Vogt T. Induction of Hsp90 protein expression in malignant melanomas and melanoma metastases. *Exp Dermatol* 2004;13(1):27–32.
- [5]. Cheng CF, Fan J, Fedesco M, Guan S, Li Y, Bandyopadhyay B, Bright AM, Yerushalmi D, Liang M, Chen M, Han YP, Woodley DT, Li W. Transforming growth factor alpha (TGFalpha)-stimulated secretion of HSP90alpha: using the receptor LRP-1/CD91 to promote human skin cell migration against a TGFbeta-rich environment during wound healing. *Mol Cell Biol* 2008;28(10):3344–3358. [PubMed: 18332123]
- [6]. Collins CB, Aherne CM, Yeckes A, Pound K, Eltzschig HK, Jedlicka P, de Zoeten EF. Inhibition of N-terminal ATPase on HSP90 attenuates colitis through enhanced Treg function. *Mucosal Immunol* 2013;6(5):960–971. [PubMed: 23321985]
- [7]. Crowe LB, Hughes PF, Alcorta DA, Osada T, Smith AP, Totzke J, Loiselle DR, Lutz ID, Gargsha M, Roy D, Roques J, Darr D, Lyerly HK, Spector NL, Haystead TAJ. A Fluorescent Hsp90 Probe Demonstrates the Unique Association between Extracellular Hsp90 and Malignancy in Vivo. *ACS Chem Biol* 2017;12(4):1047–1055. [PubMed: 28103010]
- [8]. Dixon WJ. Efficient analysis of experimental observations. *Annual review of pharmacology and toxicology* 1980;20:441–462.
- [9]. Fehrenbacher JC, Vasko MR, Duarte DB. Models of inflammation: Carrageenan- or complete Freund's Adjuvant (CFA)-induced edema and hypersensitivity in the rat. *Curr Protoc Pharmacol* 2012;Chapter 5:Unit5 4.
- [10]. Fillingim RB, Edwards RR, Powell T. The relationship of sex and clinical pain to experimental pain responses. *Pain* 1999;83(3):419–425. [PubMed: 10568849]
- [11]. Gaskin DJ, Richard P. The economic costs of pain in the United States. *J Pain* 2012;13(8):715–724. [PubMed: 22607834]
- [12]. Hargreaves K, Dubner R, Brown F, Flores C, Joris J. A new and sensitive method for measuring thermal nociception in cutaneous hyperalgesia. *Pain* 1988;32(1):77–88. [PubMed: 3340425]
- [13]. Hughes PF, Barrott JJ, Carlson DA, Loiselle DR, Speer BL, Bodoor K, Rund LA, Haystead TA. A highly selective Hsp90 affinity chromatography resin with a cleavable linker. *Bioorg Med Chem* 2012;20(10):3298–3305. [PubMed: 22520629]
- [14]. Hutchinson MR, Ramos KM, Loram LC, Wieseler J, Sholar PW, Kearney JJ, Lewis MT, Crysdale NY, Zhang Y, Harrison JA, Maier SF, Rice KC, Watkins LR. Evidence for a role of heat shock protein-90 in toll like receptor 4 mediated pain enhancement in rats. *Neuroscience* 2009;164(4):1821–1832. [PubMed: 19788917]

- [15]. Ji RR, Baba H, Brenner GJ, Woolf CJ. Nociceptive-specific activation of ERK in spinal neurons contributes to pain hypersensitivity. *Nat Neurosci* 1999;2(12):1114–1119. [PubMed: 10570489]
- [16]. Ji RR, Gereau RWt, Malcangio M, Strichartz GR. MAP kinase and pain. *Brain Res Rev* 2009;60(1):135–148. [PubMed: 19150373]
- [17]. Kaneko K, Osada T, Morse MA, Gwin WR, Ginzler JD, Snyder JC, Yang XY, Liu CX, Diniz MA, Bodoor K, Hughes PF, Haystead TA, Lyerly HK. Heat shock protein 90-targeted photodynamic therapy enables treatment of subcutaneous and visceral tumors. *Commun Biol* 2020;3(1):226. [PubMed: 32385408]
- [18]. Lei W, Mullen N, McCarthy S, Brann C, Richard P, Cormier J, Edwards K, Bilsky EJ, Streicher JM. Heat-shock protein 90 (Hsp90) promotes opioid-induced anti-nociception by an ERK mitogen-activated protein kinase (MAPK) mechanism in mouse brain. *Journal of Biological Chemistry* 2017;292(25):10414–10428. [PubMed: 28450396]
- [19]. Lei W, Mullen N, McCarthy S, Brann C, Richard P, Cormier J, Edwards K, Bilsky EJ, Streicher JM. Heat-shock protein 90 (Hsp90) promotes opioid-induced anti-nociception by an ERK mitogen-activated protein kinase (MAPK) mechanism in mouse brain. *J Biol Chem* 2017;292(25):10414–10428. [PubMed: 28450396]
- [20]. Lilja A, Weeden CE, McArthur K, Nguyen T, Donald A, Wong ZX, Dousha L, Bozinovski S, Vlahos R, Burns CJ, Asselin-Labat ML, Anderson GP. HSP90 inhibition suppresses lipopolysaccharide-induced lung inflammation in vivo. *PLoS One* 2015;10(1):e0114975. [PubMed: 25615645]
- [21]. Max MB, Payne R, Edwards WT. Principles of analgesic use in the treatment of acute pain and cancer pain 4th ed. Glenview, IL, 1999.
- [22]. Nascimento DSM, Potes CS, Soares ML, Ferreira AC, Malcangio M, Castro-Lopes JM, Neto FLM. Drug-Induced HSP90 Inhibition Alleviates Pain in Monoarthritic Rats and Alters the Expression of New Putative Pain Players at the DRG. *Mol Neurobiol* 2018;55(5):3959–3975. [PubMed: 28550532]
- [23]. Pearl LH, Prodromou C. Structure and mechanism of the Hsp90 molecular chaperone machinery. *Annu Rev Biochem* 2006;75:271–294. [PubMed: 16756493]
- [24]. Percie du Sert N, Hurst V, Ahluwalia A, Alam S, Avey MT, Baker M, Browne WJ, Clark A, Cuthill IC, Dirnagl U, Emerson M, Garner P, Holgate ST, Howells DW, Karp NA, Lazic SE, Lidster K, MacCallum CJ, Macleod M, Pearl EJ, Petersen OH, Rawle F, Reynolds P, Rooney K, Sena ES, Silberberg SD, Steckler T, Würbel H. The ARRIVE guidelines 2.0: Updated guidelines for reporting animal research. *PLoS Biol* 2020;18(7):e3000410. [PubMed: 32663219]
- [25]. Ren K, Dubner R. Inflammatory Models of Pain and Hyperalgesia. *ILAR J* 1999;40(3):111–118. [PubMed: 11406689]
- [26]. Rice JW, Veal JM, Fadden RP, Barabasz AF, Partridge JM, Barta TE, Dubois LG, Huang KH, Mabbett SR, Silinski MA, Steed PM, Hall SE. Small molecule inhibitors of Hsp90 potentially affect inflammatory disease pathways and exhibit activity in models of rheumatoid arthritis. *Arthritis Rheum* 2008;58(12):3765–3775. [PubMed: 19035474]
- [27]. Sarzi-Puttini P, Vellucci R, Zuccaro SM, Cherubino P, Labianca R, Fornasari D. The appropriate treatment of chronic pain. *Clinical drug investigation* 2012;32 Suppl 1:21–33.
- [28]. Scholz J, Woolf CJ. The neuropathic pain triad: neurons, immune cells and glia. *Nat Neurosci* 2007;10(11):1361–1368. [PubMed: 17965656]
- [29]. Shimp SK 3rd, Parson CD, Regna NL, Thomas AN, Chafin CB, Reilly CM, Nichole Rylander M. HSP90 inhibition by 17-DMAG reduces inflammation in J774 macrophages through suppression of Akt and nuclear factor-kappaB pathways. *Inflamm Res* 2012;61(5):521–533. [PubMed: 22327510]
- [30]. Sidera K, Gaitanou M, Stellas D, Matsas R, Patsavoudi E. A critical role for HSP90 in cancer cell invasion involves interaction with the extracellular domain of HER-2. *J Biol Chem* 2008;283(4):2031–2041. [PubMed: 18056992]
- [31]. Sidera K, Patsavoudi E. Extracellular HSP90: conquering the cell surface. *Cell Cycle* 2008;7(11):1564–1568. [PubMed: 18469526]
- [32]. Stine C, Coleman DL, Flohrschutz AT, Thompson AL, Mishra S, Blagg BS, Largent-Milnes TM, Lei W, Streicher JM. Heat shock protein 90 inhibitors block the antinociceptive effects

of opioids in mouse chemotherapy-induced neuropathy and cancer bone pain models. *Pain* 2020;161(8):1798–1807. [PubMed: 32701840]

- [33]. Thuringer D, Hammann A, Benikhlef N, Fourmaux E, Bouchot A, Wettstein G, Solary E, Garrido C. Transactivation of the epidermal growth factor receptor by heat shock protein 90 via Toll-like receptor 4 contributes to the migration of glioblastoma cells. *J Biol Chem* 2011;286(5):3418–3428. [PubMed: 21127066]
- [34]. Triantafilou K, Triantafilou M, Ladha S, Mackie A, Dedrick RL, Fernandez N, Cherry R. Fluorescence recovery after photobleaching reveals that LPS rapidly transfers from CD14 to hsp70 and hsp90 on the cell membrane. *J Cell Sci* 2001;114(Pt 13):2535–2545. [PubMed: 11559761]
- [35]. Triantafilou M, Triantafilou K. Heat-shock protein 70 and heat-shock protein 90 associate with Toll-like receptor 4 in response to bacterial lipopolysaccharide. *Biochem Soc Trans* 2004;32(Pt 4):636–639. [PubMed: 15270695]
- [36]. Tsen F, Bhatia A, O'Brien K, Cheng CF, Chen M, Hay N, Stiles B, Woodley DT, Li W. Extracellular heat shock protein 90 signals through subdomain II and the NPVY motif of LRP-1 receptor to Akt1 and Akt2: a circuit essential for promoting skin cell migration in vitro and wound healing in vivo. *Mol Cell Biol* 2013;33(24):4947–4959. [PubMed: 24126057]
- [37]. Urban MJ, Li C, Yu C, Lu Y, Krise JM, McIntosh MP, Rajewski RA, Blagg BS, Dobrowsky RT. Inhibiting heat-shock protein 90 reverses sensory hypoalgesia in diabetic mice. *ASN Neuro* 2010;2(4):e00040. [PubMed: 20711301]
- [38]. Urban MJ, Pan P, Farmer KL, Zhao H, Blagg BS, Dobrowsky RT. Modulating molecular chaperones improves sensory fiber recovery and mitochondrial function in diabetic peripheral neuropathy. *Exp Neurol* 2012;235(1):388–396. [PubMed: 22465570]
- [39]. Wax S, Piecyk M, Maritim B, Anderson P. Geldanamycin inhibits the production of inflammatory cytokines in activated macrophages by reducing the stability and translation of cytokine transcripts. *Arthritis Rheum* 2003;48(2):541–550. [PubMed: 12571865]
- [40]. Wiech H, Buchner J, Zimmermann R, Jakob U. Hsp90 chaperones protein folding in vitro. *Nature* 1992;358(6382):169–170. [PubMed: 1614549]
- [41]. Xu S, Cheng Y, Keast JR, Osborne PB. 17beta-estradiol activates estrogen receptor beta-signalling and inhibits transient receptor potential vanilloid receptor 1 activation by capsaicin in adult rat nociceptor neurons. *Endocrinology* 2008;149(11):5540–5548. [PubMed: 18617618]
- [42]. Xu ZZ, Kim YH, Bang S, Zhang Y, Berta T, Wang F, Oh SB, Ji RR. Inhibition of mechanical allodynia in neuropathic pain by TLR5-mediated A-fiber blockade. *Nature medicine* 2015;21(11):1326–1331.
- [43]. Zimmermann M Ethical guidelines for investigations of experimental pain in conscious animals. *Pain* 1983;16(2):109–110. [PubMed: 6877845]

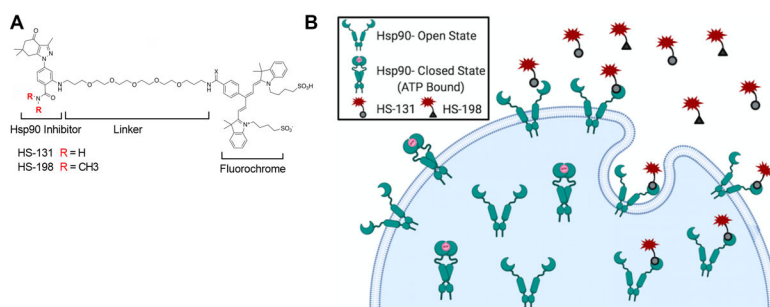


Figure 1. Selective targeted inhibition of eHsp90 function.

(A) Chemical scaffolds of the eHsp90 inhibitor HS-131 and the inactive analog HS-198 (negative control). (B) eHsp90 expressed on the cellular membrane, where it binds and internalized HS-131.

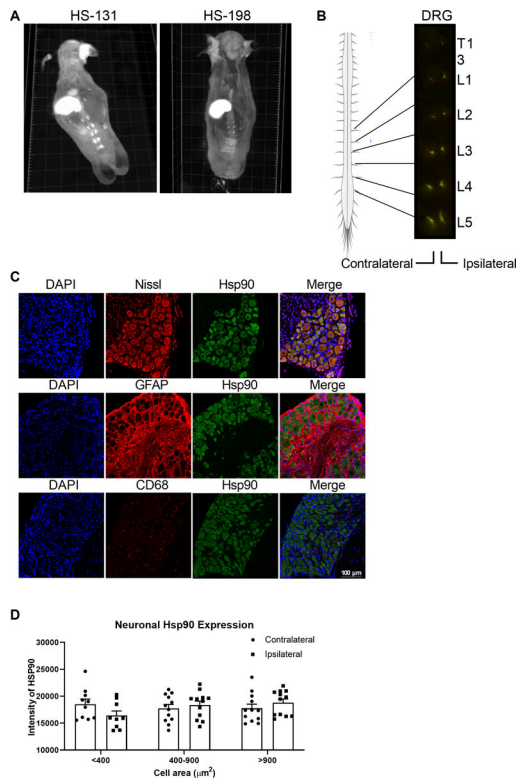


Figure 2. DRG neurons innervating sites of peripheral inflammation express eHsp90.

(A) Whole body cryo-imaging of female mice 6 hours after HS-131 treatment (10 nmoles, i.v.) on day 3 post CFA (i.pl.) reveals eHsp90 expression in lumbar DRG (B) eHsp90 expression was greatest in ipsilateral and contralateral DRG in the L3-L5 region. (C) Confocal imaging shows that CFA-induced Hsp90 expression in DRG was localized to Nissl+ neurons. (D) IHC analysis reveals Hsp90 expression is comparable in small, medium, and large neurons in both ipsilateral and contralateral DRG. N=1428 DRG neurons from 2 male mice and 1463 DRG from 2 female mice. Data are mean \pm SEM.

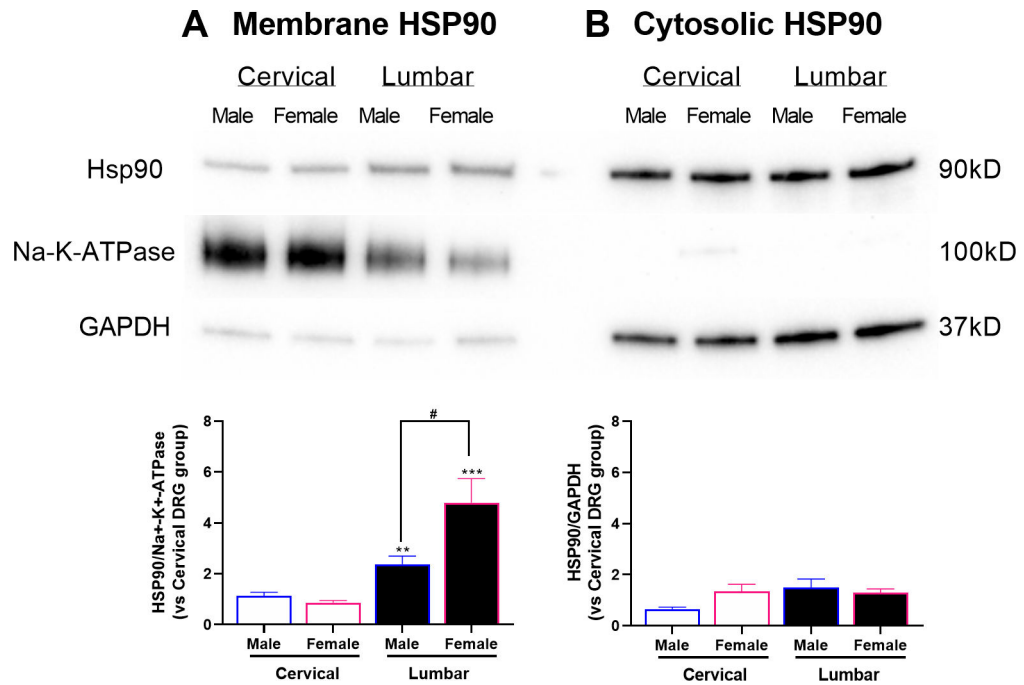


Figure 3. Intra-plantar CFA injection induces membrane Hsp90 expression in lumbar DRG, especially in females.

(A) CFA-induced membrane-bound eHsp90 expression was higher in lumbar DRG compared to control cervical DRG. Further, eHsp90 expression was higher in females than males. (B) Cytosolic Hsp90 expression did not differ between lumbar and cervical DRG or between males and females. N=14 (7M, 7F) mice per group. Data are mean \pm SEM. ** P <0.01 different from cervical. # P <0.05 different from males.

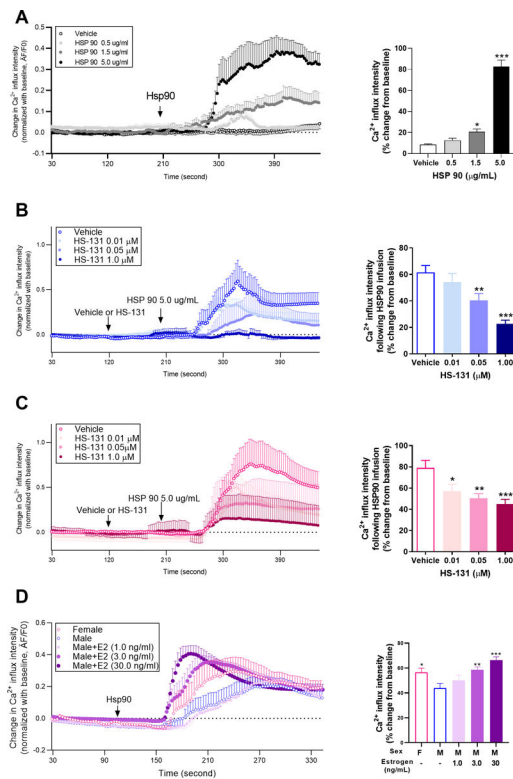


Figure 4. Exogenous Hsp90 induces calcium influx in primary afferent nociceptors. (A) Calcium traces and analysis of group differences in primary DRG nociceptors isolated from Pirt-GCaMP3 mice following *ex vivo* stimulation with Hsp90 show that Hsp90 dose-dependently increases calcium responses. N=5 (2M, 3F) mice per group. (B) Administration of HS-131 prior to Hsp90, dose-dependently decreases calcium responses in males. N=5M mice per group. (C) Administration of HS-131 prior to Hsp90, dose-dependently decreases calcium responses in females N=5M mice per group. (D) Female primary nociceptors exhibit greater calcium responses to Hsp90 compared to male primary nociceptors. Incubation of male primary DRG nociceptors with estrogen overnight at varying concentrations enhances calcium response to exogenous Hsp90 N=10 (8M, 2F) mice per group. Data are mean \pm SEM. * P <0.05, ** P <0.01, *** P <0.001 different from vehicle in Panels A, B, and C and different from males in Panel D.

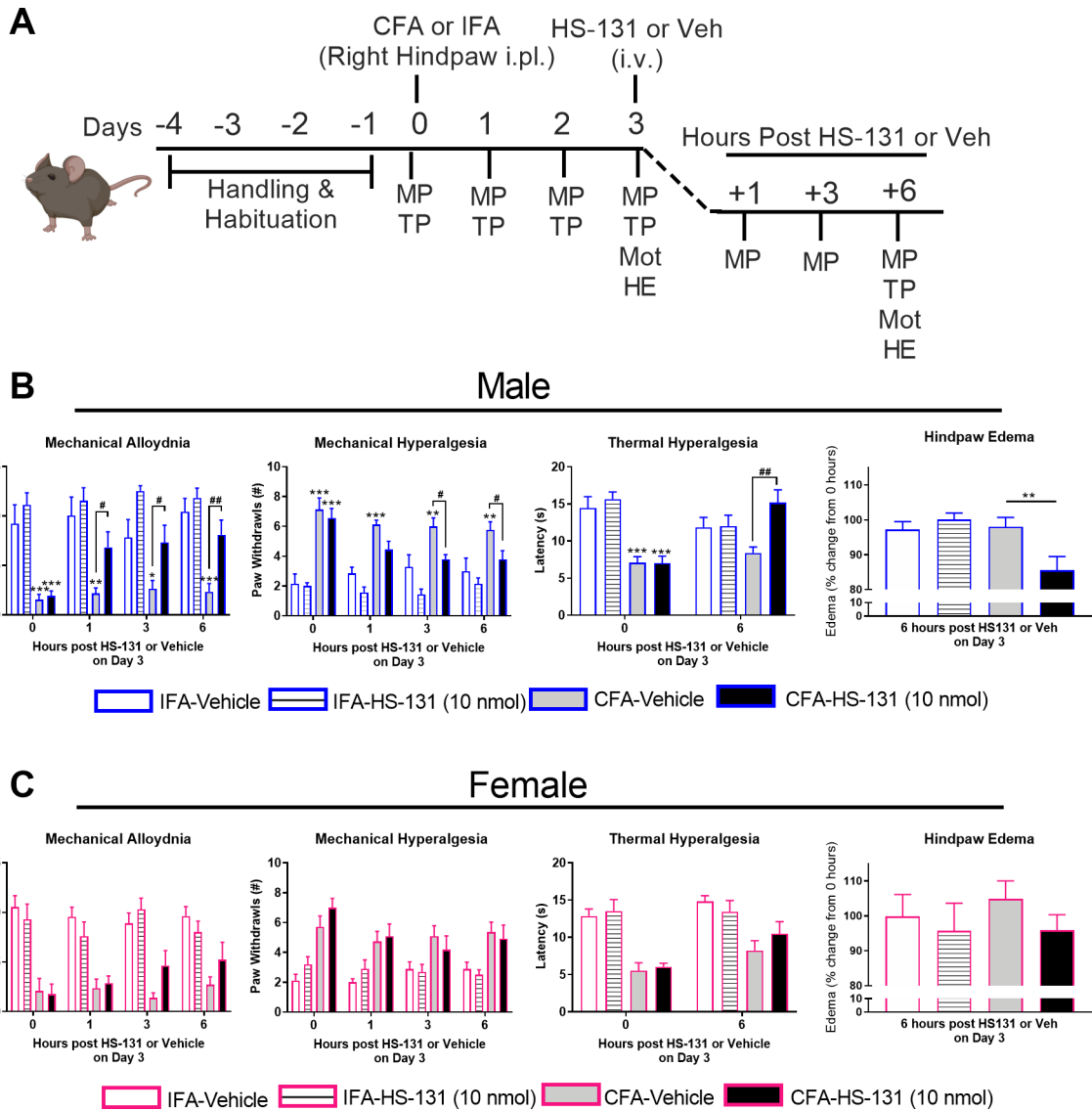


Figure 5. Inhibition of eHsp90 with HS-131 (10 nmols) alleviates CFA-induced pain and inflammation in male, but not female mice.

(A) Experimental timeline. Mechanical pain (MP), thermal pain (TP), and motor function (Mot) were evaluated prior to CFA/IFA administration on days 1, 2 and 3 post CFA/IFA, and at hours 1, 3, and 6 after HS-131/Veh. Hindpaw edema (HE) was measured on day 3 prior to and 6 hours after HS-131/Veh. (B) Administration of HS-131 (10 nmol) attenuated CFA-induced mechanical allodynia, mechanical hyperalgesia, thermal heat hyperalgesia and edema in male mice. (C) In contrast, administration of HS-131 (10 nmol) had no significant effect on pain and hindpaw edema in female mice. IFA-Veh N=18 (7M, 11F), IFA-HS131 N=17 (7M, 11F), CFA-Veh N=20 (9M, 11F), and CFA-HS131 N=20 (9M, 11F) mice. For edema, IFA-Veh N=9 (5M, 4F), IFA-HS131 N=10 (5M, 5F), CFA-Veh N=12 (5M, 7F), and CFA-HS131 N=12 (5M, 7F) mice. Data are mean \pm SEM. * P <0.05, ** P <0.01, *** P <0.001 different from IFA controls. # P <0.05, ## P <0.01 different from CFA-Veh.

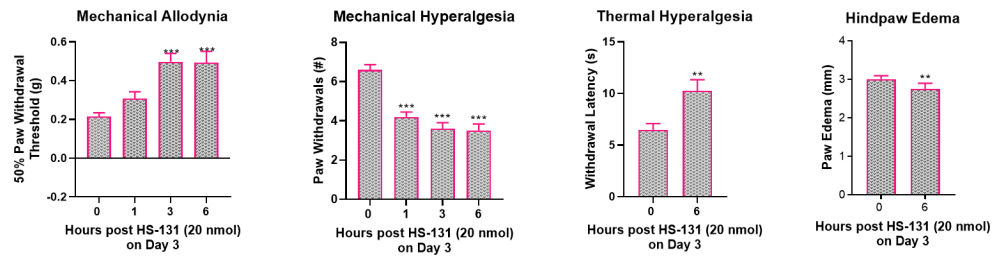


Figure 6. A higher dose of HS-131 (20 nmol) alleviates CFA- induced pain and inflammation in female mice.

Administration of HS-131 (20 nmols) significantly reduced mechanical allodynia, mechanical hyperalgesia, thermal heat hyperalgesia, and hindpaw edema after treatment on day 3 post CFA. N=10 mice per group. Data are mean \pm SEM. ** $P < 0.01$, *** $P < 0.001$ different from hour 0 prior to HS-131.